Quaternary International 386 (2015) 18–29

Contents lists available at ScienceDirect

Quaternary International

journal homepage: www.elsevier.com/locate/quaint

Geochemical evidence of the presence of volcanic and meteoritic materials in Late Pleistocene lake sediments of Lithuania

Alexandre V. Andronikov [a, *], Eugenija Rudnickaitė [b], Dante S. Lauretta [a], Irina E. Andronikova [a], Donatas Kaminskas [b], Petras Šinkūnas [b], Monika Melešytė [b]

[a] Lunar and Planetary Laboratory, University of Arizona, Tucson, AZ 85721, USA
[b] Department of Geology and Mineralogy, Vilnius University, M.K. Čiurlionio 21/27, LT-03101, Vilnius, Lithuania

ARTICLE INFO

Article history:
Available online 1 November 2014

Keywords:
Late Pleistocene
Lithuania
Meteoritic and volcanic materials
Sediments
Trace-elements

ABSTRACT

Concentrations of trace elements in four Late Pleistocene lake sediment sequences across Lithuania were studied using inductively coupled plasma-mass spectrometry (ICP-MS). Such elements as Cr, Cu, Eu, La, Ni, Zn, Zr, and platinum group elements were used for constraints. The studied sediments deposited during the time interval from Bølling to Allerød and to Younger Dryas. Material for sediments of the Dengtiltis and Krokšlys sequences was delivered from the same or very similar source. Geochemical features of the sediments are consistent with the presence of extraterrestrial material in at least two horizons separated by ~2000 years, and resulted from two separate events. The younger horizon is detected in all studied sequences and corresponds to the age of ca. 11.0–11.5 ka BP. Its geochemical features are suggested to result from a local meteorite impact/bolide explosion tentatively related to the Velnio Duobės meteorite crater. The older horizon detected only for the Ūla-2 sequence corresponds to the age of ca. 13.5 ka BP and is due to the bolide airburst. There is also suggested meteoritic material in sediments dated as ca. 12.9 ka BP. The presence of volcanic materials related to the volcanic activity in the French Massif Central (a volcano of ca. 15.3 ka BP), and Laacher See volcano in Germany (12.88 ka BP) are suggested for some sedimentary layers of the studied sequences.

1. Introduction

In the Northern Hemisphere, the last glacial–interglacial transition ended with the beginning of the cold period known as the Younger Dryas (YD) climate oscillation, which occurred between 12.9 and 11.7 ka BP (e.g., Peteet, 1995; Alley, 2000; Björck, 2007; Lowe et al., 2008). This climate oscillation is generally thought to result from an abrupt change of atmospheric and oceanic circulation (e.g., Berger, 1990; Teller et al., 2002; McManus et al., 2004; Brauer et al., 2008; Murton et al., 2010). However, there are other hypotheses including such as that proposed by Firestone et al. (2007). This hypothesis suggests that just before the onset of the YD cooling (ca. 12.9–12.8 ka BP), a large bolide exploded over the North American Laurentide Ice Shield, and consequences of such a catastrophic event ("meteorite impact winter") led to a global climate change. Suggestions about both the extraterrestrial (ET) event itself and its influence on the Earth's climate resulted in a wide-spread discussion, which has yet to result in a decisive conclusion (see Pinter et al., 2011; Bunch et al., 2012; Israde-Alcántara et al., 2012; LeCompte et al., 2012; Wittke et al., 2013; Wu et al., 2013; van Hoesel et al., 2014 for details).

If the Late Pleistocene ET event occurred over North America, transportation of the related microparticles eastward by the dominating west winds (e.g., Isarin and Renssen, 1999; Brauer et al., 2008) could result in distal fallout from the impact/airburst cloud as far as Europe (cf. Bunch et al., 2008; Artemieva and Morgan, 2009). However, the studies of the YD impact hypothesis in Europe are so far very limited (e.g., Beets et al., 2008; Tian et al., 2010; Marshall et al., 2011; van Hoesel et al., 2012, 2014; Wu et al., 2013; Andronikov et al., 2014). In order to extend our knowledge about the possible presence of the ET material in the Late Pleistocene sediments of Europe, we conducted geochemical analyses of sediments in sequences from four localities in Lithuania (Fig. 1). This way, it is possible to decipher the trace element distribution across the sequences and to detect the presence of anomalous (in particular, ET-related) components.

* Corresponding author.
E-mail address: andron@lpl.arizona.edu (A.V. Andronikov).

http://dx.doi.org/10.1016/j.quaint.2014.10.005
1040-6182/

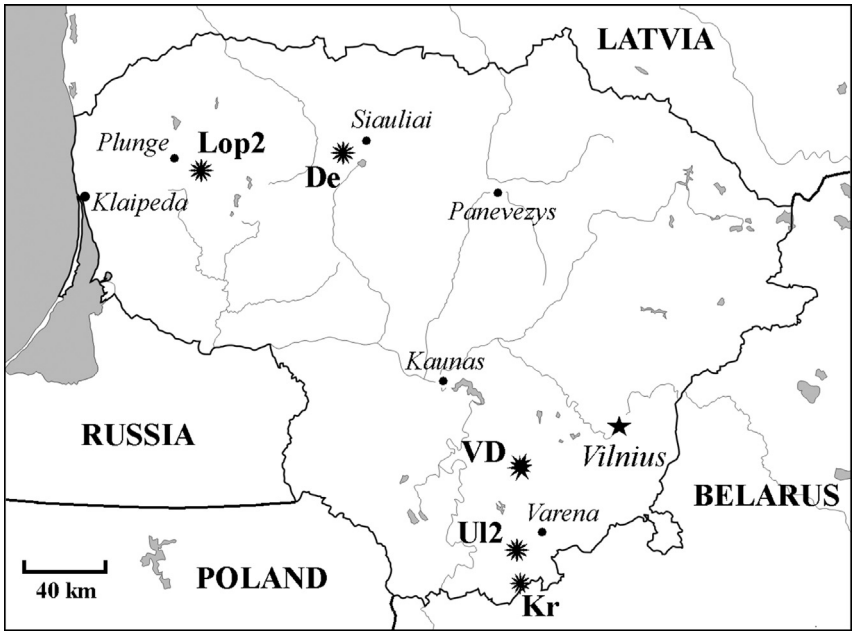

Fig. 1. A map showing the location of the studied sedimentary sequences in Lithuania (black asterisks). De, Dengtiltis outcrop; Lop2, Lopaičiai-2 drilling site; Kr, Krokšlys outcrop; Ul2, Ūla-2 outcrop; VD, Velnio Duobės structure.

2. Materials and methods

2.1. Study sites

Late Pleistocene lake sediments were collected from four sites across Lithuania: Dengtiltis outcrop located ~20 km SW of Šiauliai at N 55°46′16″ and E 23°07′08″ on an abrupt bend of Dubysa River; Lopaičiai-2 drilling site located ~30 km SE of Plungė at N 55°44′38″ and E 22°11′34″ in a little hollow on a hill of 210 m a.s.l.; Krokšlys outcrop located ~10 km SW from Varėna at N 54°02′31″ and E 22°37′58″ on the left bank of the Ūla River; and Ūla-2 outcrop located ~20 km SW from Varėna at N 54°06′34″ and E 24°28′44″, also on the left bank of the Ūla River (Fig. 1). Ūla is a river in Dzūkija National Park in southern Lithuania flowing across various aeolian relief forms.

The studied part of the Dengtiltis sequence (Fig. 2a) is lithologically homogeneous and represented by fine yellowish to brownish carbonaceous sand. The studied part of the Lopaičiai-2 sequence (Fig. 2b) is lithologically inhomogeneous and consists of three different parts: the lower to middle part of the section is represented by fine yellowish sand, the middle to upper part by dark-grey clay with thin interlayers of gyttja, and the uppermost part by peat. The studied part of the Krokšlys sequence (Fig. 2c) is also inhomogeneous and consists of yellowish sand at the lowermost studied levels, peat in the middle part of the section, and fine aeolian sand at the middle to uppermost levels. The studied part of the Ūla-2 sequence (Fig. 2d) is inhomogeneous, displaying yellowish (limonitized) sand at the lowermost studied levels, and gyttja with mollusk shells for the rest of the studied part of the sequence, which becomes silty clay at the uppermost levels.

2.2. Sample preparation and analytical techniques

A few grams of material from each sample were dried overnight at 105 °C and then pulverized in an agate mortar. Approximately 50 mg of the pulverized material from each sample were digested in a mixture of concentrated HNO_3 and HF in 15 ml Teflon beakers. The beakers were sealed and heated on a hot plate at 130 °C for 48 h during which time they were ultrasonicated twice. After cooling, this solution was dried down and then brought back to the solution with 5% HNO_3. Visual inspection revealed that the samples completely dissolved. The solutions yielded approximately 100 μg/ml of total dissolved solids for further analyses for most trace elements and 300 μg/ml for platinum group elements (PGE) because of general very low PGE concentrations in terrestrial sediments. For this pilot study, we needed only to recognize features of the PGE behavior in different samples. Therefore, we did not conduct PGE enrichment with the use of column chromatography, but instead analyzed the bulk samples as they are in order to compare PGE signal intensities from different samples on the ICP-MS spectra. For the PGE, we additionally analyzed aliquots of marls from Murray Springs, Arizona (USA), which are similar in concentrations to the Average Continental Crust (ACC; Wedepohl, 1995) (authors' unpublished data). Samples signal intensities were corrected to the sample mass and then normalized to the marls (≈ACC) intensity. Rhenium-185 was monitored as an internal standard during the PGE runs. The following isotopes were monitored during the analytical runs: P^{31}, Sc^{45}, Ti^{47}, V^{51}, Cr^{52}, Co^{59}, Ni^{60}, Cu^{63}, Zn^{66}, Rb^{85}, Sr^{87}, Sr^{88}, Y^{89}, Zr^{90}, Nb^{93}, Ru^{101}, Rh^{103}, Pd^{104}, Pd^{105}, Sn^{118}, Cs^{133}, Ba^{137}, La^{139}, Ce^{140}, Pr^{141}, Nd^{144}, Nd^{146}, Sm^{147}, Eu^{153}, Gd^{157}, Tb^{159}, Dy^{163}, Ho^{165}, Er^{166}, Tm^{169}, Yb^{172}, Lu^{175}, Hf^{178}, Ta^{181}, W^{182}, Re^{185}, Os^{189}, Os^{192}, Ir^{193}, Pt^{195}, Pb^{206}, Pb^{208}, Th^{232}, and U^{238}. Analyses were run in a low resolution mode for all isotopes and additionally in a medium resolution mode for P^{31}, Sc^{45}, Ti^{47}, V^{51}, Cr^{52}, Co^{59}, Ni^{60}, Cu^{63}, and Zn^{66}. An analytical blank solution was prepared using the same procedure. A Finnigan Element2 inductively coupled plasma-mass spectrometer (ICP-MS) was used for analysis. Solution standards consisted of known amounts of the analyzed elements and were prepared using multi-element solutions obtained from High-Purity Standards (Charleston, SC, USA). Sample concentrations were determined by first subtracting blank signal intensities from those obtained from the sample and standard solutions. A calibration curve was obtained by performing a linear least-squares regression for each element using the blank-subtracted counts and the known

concentrations in each standard solution. In all cases, the regression coefficients were 0.998 or higher.

3. Analytical results

All analytical results are summarized in Table 1, and graphically depicted in Figs. 3–10.

Table 1
Trace element composition of Lithuanian samples (ppm).

	Dengtiltis						
	De-11	De-12	De-13	De-14	De-15	De-16	De-17
	450 cm	443 cm	430 cm	425 cm	422 cm	410 cm	400 cm
P	n.d.	n.d.	n.d.	n.d.	n.d.	n.d.	n.d.
Sc	2.332	1.821	1.575	2.328	1.870	1.528	1.703
Ti	853.7	764.8	897.5	881.9	768.2	799.9	743.3
V	9.862	8.266	7.631	12.79	9.897	8.229	7.909
Cr	7.005	6.083	5.465	9.843	7.039	6.187	5.785
Co	3.239	3.955	2.877	3.521	4.028	5.003	5.037
Ni	4.451	4.229	3.374	4.534	3.308	20.50	12.87
Cu	6.193	5.427	4.374	8.250	8.917	5.083	4.536
Zn	18.57	13.85	10.69	13.68	14.18	13.64	13.48
Rb	35.29	48.10	32.33	37.50	45.32	41.68	44.33
Sr	62.49	80.17	62.91	62.67	80.17	73.89	77.43
Y	7.858	8.182	7.335	7.897	7.916	7.513	8.745
Zr	86.57	69.25	86.01	66.41	66.33	87.87	98.12
Nb	2.607	2.388	2.666	2.983	2.298	2.029	2.392
Sn	0.893	0.915	0.813	0.740	0.909	0.798	0.921
Cs	0.594	0.666	0.489	0.743	0.752	0.552	0.681
Ba	229.3	316.1	216.1	221.6	295.7	271.1	299.8
La	10.47	9.46	8.36	9.14	11.14	7.203	10.85
Ce	22.55	20.89	18.78	20.03	22.57	15.80	22.47
Pr	2.604	2.387	2.017	2.316	2.793	1.816	2.718
Nd	10.26	9.505	8.058	9.251	11.26	7.284	10.83
Sm	2.031	1.903	1.633	1.900	2.313	1.533	2.187
Eu	0.545	0.647	0.495	0.539	0.692	0.492	0.638
Gd	2.009	1.854	1.562	1.858	2.312	1.531	2.119
Tb	0.318	0.304	0.268	0.318	0.350	0.265	0.350
Dy	1.549	1.546	1.411	1.582	1.622	1.409	1.742
Ho	0.314	0.325	0.293	0.319	0.319	0.292	0.355
Er	0.994	1.020	0.925	0.988	0.966	0.907	1.089
Tm	0.145	0.147	0.135	0.136	0.127	0.131	0.150
Yb	1.066	1.016	0.929	0.925	0.872	0.901	1.014
Lu	0.163	0.157	0.145	0.139	0.131	0.140	0.153
Hf	2.563	2.138	2.888	2.006	2.061	3.073	2.980
Ta	0.222	0.216	0.243	0.256	0.205	0.216	0.220
W	0.257	0.309	0.235	0.301	0.287	0.230	0.264
Pb	7.012	8.933	6.600	7.300	9.440	8.283	8.653
Th	3.202	2.266	2.087	2.612	2.859	2.028	3.343
U	0.798	0.732	0.736	0.736	0.849	0.796	0.868
	Lopaičiai-2							
	Lop2-25	Lop2-26	Lop2-30	Lop2-35	Lop2-37	Lop2-38	Lop2-39	Lop2-41
	175 cm	180 cm	190 cm	200 cm	210 cm	220 cm	230 cm	240 cm
P	482.8	665.3	775.9	503.9	616.3	409.5	399.2	494.8
Sc	2.532	3.539	5.898	5.233	6.110	5.169	6.234	5.811
Ti	422.6	616.9	2116	1954	2220	1784	2161	2014
V	15.22	21.44	33.63	36.05	41.57	41.34	43.96	42.54
Cr	14.56	18.69	30.41	30.65	33.21	27.50	34.00	32.12
Co	2.392	1.065	2.854	4.721	5.167	7.581	10.05	10.40
Ni	5.808	6.616	8.625	12.32	9.933	25.08	21.22	23.91
Cu	42.01	61.08	16.04	13.35	19.40	12.10	16.52	15.41
Zn	60.43	220.6	62.88	64.91	85.22	133.5	62.00	82.22
Rb	12.31	21.23	74.08	64.40	68.26	61.09	73.45	66.69
Sr	32.50	117.3	74.39	66.33	70.85	63.70	70.34	65.21
Y	6.557	10.33	13.94	15.33	14.98	19.38	18.72	19.14
Zr	19.77	25.70	152.0	182.0	124.0	120.9	135.9	148.1
Nb	1.522	2.105	6.372	6.156	6.504	5.383	6.538	6.382
Sn	0.215	0.376	1.109	0.886	1.104	0.891	1.098	1.009
Cs	0.736	1.205	2.161	1.924	2.177	1.817	2.372	2.084
Ba	79.24	101.4	385.6	347.4	368.9	302.3	337.2	307.5

Table 1 (*continued*)

	Lopaičiai-2							
	Lop2-25	Lop2-26	Lop2-30	Lop2-35	Lop2-37	Lop2-38	Lop2-39	Lop2-41
	175 cm	180 cm	190 cm	200 cm	210 cm	220 cm	230 cm	240 cm
La	8.366	13.42	19.38	22.34	22.35	26.99	24.87	26.00
Ce	16.84	25.39	39.60	47.92	46.18	57.96	52.99	56.39
Pr	1.916	3.025	4.695	5.523	5.426	6.790	6.200	6.565
Nd	7.453	11.84	18.01	20.88	20.64	26.13	24.42	25.38
Sm	1.472	2.318	3.520	4.144	4.050	5.092	4.726	5.027
Eu	0.337	0.521	0.971	0.925	1.008	1.127	1.119	1.165
Gd	1.562	2.478	3.632	4.379	4.155	5.338	5.080	5.647
Tb	0.244	0.391	0.603	0.666	0.669	0.837	0.789	0.843
Dy	1.170	1.874	2.889	3.126	3.142	3.828	3.678	3.820
Ho	0.231	0.371	0.567	0.612	0.608	0.746	0.718	0.744
Er	0.729	1.131	1.808	1.939	1.896	2.376	2.272	2.375
Tm	0.094	0.147	0.254	0.260	0.255	0.311	0.303	0.315
Yb	0.628	0.965	1.779	1.775	1.735	2.086	2.055	2.133
Lu	0.091	0.142	0.270	0.272	0.259	0.309	0.311	0.323
Hf	0.586	0.795	4.533	5.049	3.651	3.566	4.094	4.322
Ta	0.105	0.146	0.482	0.461	0.490	0.399	0.515	0.478
W	10.55	0.455	1.345	8.175	0.554	0.576	0.785	5.317
Pb	3.833	5.986	16.75	14.98	16.62	13.88	16.22	15.26
Th	2.383	3.413	6.468	7.733	6.712	6.869	6.984	6.897
U	1.056	1.827	2.427	2.158	2.285	2.004	2.310	2.449
	Lopaičiai-2			Krokšlys				
	Lop2-43	Lop2-45	Lop2-46	Kr-127	Kr-128	Kr-129	Kr-131	Kr-132
	250 cm	260 cm	270 cm	195 cm	185 cm	175 cm	155 cm	145 cm
P	530.0	320.5	311.0	n.d.	n.d.	n.d.	n.d.	n.d.
Sc	6.391	3.822	3.465	1.211	1.075	1.077	1.366	1.069
Ti	2067	1174	1174	815.9	798.6	750.4	761.4	848.4
V	43.90	26.15	19.11	6.693	7.000	6.041	6.238	5.967
Cr	33.88	21.27	19.59	6.065	5.752	5.280	7.100	4.628
Co	10.18	6.033	4.101	1.101	0.758	0.810	0.719	0.780
Ni	20.42	11.51	8.638	2.239	2.242	1.999	2.538	1.744
Cu	17.02	10.19	7.854	2.876	1.669	2.527	0.723	0.849
Zn	92.73	74.04	58.57	13.75	11.59	9.661	9.599	8.872
Rb	68.58	59.05	55.01	27.63	30.89	29.91	28.25	25.22
Sr	68.25	69.13	70.79	30.20	33.36	34.65	31.07	27.42
Y	18.59	10.95	10.93	3.687	3.215	3.932	4.803	4.076
Zr	132.3	70.59	101.5	61.06	42.00	67.73	80.69	45.06
Nb	7.794	3.767	3.387	2.932	2.005	2.123	2.083	2.031
Sn	1.076	0.701	0.638	0.286	0.275	0.275	0.283	0.176
Cs	2.300	1.644	1.238	0.592	0.590	0.646	0.559	0.484
Ba	305.7	288.4	291.8	183.1	211.6	226.8	204.1	177.2
La	26.90	14.71	13.22	6.004	6.825	8.158	7.012	7.047
Ce	58.51	29.70	27.08	12.70	13.95	16.83	14.62	14.58
Pr	6.779	3.461	3.182	1.384	1.528	1.890	1.627	1.611
Nd	25.53	13.23	12.26	5.116	5.620	6.943	6.070	5.925
Sm	4.960	2.613	2.415	0.972	1.036	1.182	1.124	1.069
Eu	1.109	0.757	0.730	0.325	0.348	0.341	0.344	0.285
Gd	5.167	2.726	2.624	1.004	1.101	1.291	1.166	1.064
Tb	0.790	0.444	0.423	0.152	0.158	0.184	0.185	0.173
Dy	3.663	2.143	2.053	0.739	0.689	0.795	0.919	0.803
Ho	0.711	0.424	0.409	0.151	0.132	0.162	0.194	0.164
Er	2.228	1.330	1.313	0.512	0.435	0.571	0.649	0.540
Tm	0.306	0.179	0.184	0.073	0.057	0.078	0.099	0.076
Yb	2.110	1.211	1.279	0.523	0.402	0.559	0.712	0.530
Lu	0.323	0.181	0.194	0.079	0.058	0.082	0.107	0.078
Hf	3.938	2.191	2.969	1.751	1.193	1.901	2.485	1.303
Ta	0.477	0.281	0.250	0.219	0.151	0.162	0.161	0.137
W	0.623	0.382	8.169	0.166	0.169	0.176	0.168	0.154
Pb	16.01	11.03	9.741	6.417	10.97	11.68	9.364	7.807
Th	8.248	4.067	3.407	1.843	1.995	2.584	2.223	2.167
U	2.496	1.700	1.479	0.555	0.560	0.635	0.712	0.517
	Krokšlys				Ula-2			
	Kr-133	Kr-134	Kr-135	Kr-139	Ula2-49	Ula2-50	Ula2-52	Ula2-54
	135 cm	125 cm	115 cm	75 cm	610 cm	620 cm	630 cm	640 cm
P	n.d.	n.d.	n.d.	n.d.	n.d.	n.d.	n.d.	n.d.
Sc	1.074	1.255	1.093	1.137	1.353	3.283	14.63	34.07
Ti	558.4	599.2	549.4	516.9	953.1	1054	258.0	242.7
V	5.640	5.995	6.315	5.901	5.995	5.675	10.64	8.494
Cr	4.941	5.090	5.233	4.547	5.438	11.11	5.147	5.088

Table 1 (*continued*)

	Krokšlys				Ūla-2			
	Kr-133	Kr-134	Kr-135	Kr-139	Ula2-49	Ula2-50	Ula2-52	Ula2-54
	135 cm	125 cm	115 cm	75 cm	610 cm	620 cm	630 cm	640 cm
Co	0.853	0.762	0.751	0.912	5.781	3.731	8.807	6.429
Ni	1.918	1.778	1.964	1.772	3.866	7.467	12.57	12.82
Cu	3.747	1.211	0.975	2.853	3.961	3.533	3.599	3.617
Zn	5.613	9.305	5.251	8.374	8.877	9.650	12.52	8.988
Rb	37.78	31.20	33.01	33.63	27.78	30.17	4.537	4.173
Sr	43.00	35.48	50.11	39.81	44.10	49.36	84.96	102.4
Y	3.753	4.157	3.680	4.737	6.865	6.585	1.968	1.850
Zr	26.89	59.36	47.58	80.01	87.25	104.0	17.42	16.13
Nb	1.625	1.703	1.524	1.507	2.217	2.416	0.663	0.567
Sn	0.135	0.096	0.095	0.058	0.158	0.120	0.017	0.004
Cs	0.631	0.569	0.549	0.532	0.334	0.365	0.163	0.164
Ba	260.8	204.6	230.1	249.4	199.7	223.5	225.5	215.1
La	6.488	5.617	10.41	7.233	9.635	11.24	1.927	1.321
Ce	13.31	11.66	21.76	15.57	23.13	20.20	4.160	2.884
Pr	1.436	1.226	2.399	1.641	2.629	2.431	0.479	0.331
Nd	5.263	4.511	8.910	5.832	9.825	9.304	1.902	1.330
Sm	0.989	0.839	1.585	1.086	1.826	1.872	0.377	0.291
Eu	0.407	0.349	0.396	0.420	0.427	0.448	0.182	0.172
Gd	1.206	0.878	1.698	1.213	2.026	1.951	0.422	0.349
Tb	0.166	0.154	0.213	0.187	0.284	0.279	0.066	0.056
Dy	0.767	0.789	0.797	0.896	1.306	1.299	0.335	0.297
Ho	0.155	0.166	0.153	0.192	0.253	0.255	0.071	0.063
Er	0.520	0.540	0.532	0.656	0.797	0.817	0.224	0.198
Tm	0.071	0.078	0.066	0.097	0.108	0.110	0.031	0.028
Yb	0.483	0.523	0.464	0.692	0.749	0.769	0.210	0.191
Lu	0.069	0.077	0.066	0.104	0.113	0.116	0.032	0.029
Hf	0.7901	1.637	1.324	2.188	2.332	2.873	0.386	0.368
Ta	0.137	0.134	0.117	0.114	0.168	0.180	0.048	0.042
W	0.144	0.117	0.206	0.169	0.108	0.135	0.474	0.396
Pb	8.490	7.077	7.689	7.183	5.043	5.904	1.072	0.890
Th	1.886	1.443	2.956	1.954	2.539	2.983	0.529	0.387
U	0.441	0.464	0.645	0.521	0.742	1.064	1.339	0.507

	Ūla-2					
	Ula2-56	Ula2-58	Ula2-60	Ula2-62	Ula2-64	Ula2-66
	650 cm	660 cm	670 cm	680 cm	690 cm	700 cm
P	n.d.	n.d.	n.d.	n.d.	n.d.	n.d.
Sc	38.35	1.354	23.54	19.11	73.35	16.36
Ti	254.2	221.5	213.2	231.4	731.3	1195
V	8.407	13.04	12.45	13.13	19.65	20.34
Cr	5.238	7.076	6.557	6.237	12.50	13.74
Co	5.341	7.976	5.283	4.627	7.547	5.234
Ni	13.79	15.00	15.50	15.30	19.29	9.566
Cu	3.913	4.241	3.977	3.849	13.07	10.61
Zn	6.186	8.442	6.183	6.944	17.24	22.42
Rb	4.669	5.267	4.213	4.546	15.62	31.61
Sr	95.91	96.48	99.75	90.39	106.4	70.60
Y	1.706	1.830	1.588	1.668	5.045	9.611
Zr	15.49	15.39	14.71	13.55	37.07	96.52
Nb	0.605	0.617	0.594	0.595	1.948	3.076
Sn	0.004	0.009	0.023	0.015	0.227	0.319
Cs	0.180	0.213	0.169	0.213	0.628	0.664
Ba	207.7	258.2	251.9	251.4	203.9	392.1
La	1.616	1.815	1.832	1.642	6.006	10.19
Ce	3.439	3.846	3.899	3.481	13.18	22.21
Pr	0.390	0.442	0.442	0.396	1.485	2.563
Nd	1.540	1.731	1.743	1.566	5.810	9.926
Sm	0.311	0.347	0.341	0.317	1.164	1.998
Eu	0.174	0.200	0.188	0.204	0.338	0.618
Gd	0.375	0.401	0.382	0.360	1.277	2.123
Tb	0.054	0.059	0.055	0.053	0.187	0.336
Dy	0.286	0.298	0.267	0.269	0.911	1.690
Ho	0.061	0.064	0.054	0.057	0.185	0.345
Er	0.195	0.205	0.172	0.181	0.568	1.080
Tm	0.028	0.029	0.023	0.025	0.075	0.149
Yb	0.203	0.191	0.156	0.163	0.498	1.002
Lu	0.031	0.030	0.023	0.024	0.075	0.149
Hf	0.463	0.278	0.257	0.222	0.862	2.465
Ta	0.048	0.044	0.043	0.044	0.142	0.220
W	0.422	0.542	0.534	0.575	0.360	0.388
Pb	0.981	1.100	0.980	0.943	3.705	6.318

Table 1 (*continued*)

	Ūla-2					
	Ula2-56	Ula2-58	Ula2-60	Ula2-62	Ula2-64	Ula2-66
	650 cm	660 cm	670 cm	680 cm	690 cm	700 cm
Th	0.506	0.551	0.478	0.439	1.600	2.576
U	0.503	3.628	1.191	0.620	1.277	0.856

n.d., no data available.

3.1. Dengtiltis

Seven samples of carbonaceous sand from the depth interval of 400–455 cm were analyzed. A total amount of trace-elements in the studied samples is ~1400 ppm, which is 2–3 times lower than that in the ACC. Rare earth element (REE) patterns on a CI chondrite-normalized diagram (Fig. 3a) are similar for all samples, being moderately fractionated (Ce_N/Yb_N = 4.7–6.0), and following the pattern for the ACC, but with overall lower concentrations. An ACC-normalized trace-element diagram (Fig. 3b) shows similar patterns for most samples, which are characterized by marked troughs at Ta–Nb, Ti,Y, and, for most samples, at Co–Ni. Additionally, samples De-13 and De-16 show elevated concentration of Zr and Hf, and samples De-16 and De-17 display higher as compared to other samples amounts of Ni. Signal intensities of the PGE in the Dengtiltis sediments are slightly above the ACC PGE signal intensities except for samples from the upper part of the sequence (De-16 and De-17; 410 and 400 cm, respectively) where the PGE signal intensities increase 2–3 times (Fig. 7b).

3.2. Lopaičiai-2

Eleven samples from the depth interval of 175–270 cm were analyzed. The lowermost part of the interval (samples Lop2-45 and Lop2-46; both are fine sand) is characterized by total amounts of the trace-elements <1900 ppm, which are approximately two times lower than those in the ACC. The rest of the sandy part of the section, and the clayish part of the section are characterized by total amounts of the trace-elements of ~3000 ppm, which are comparable to the ACC concentrations. The uppermost (peat) part of the section is low in trace-elements (<1500 ppm), which are ~2.5 times lower than in the ACC. The REE patterns style on a CI chondrite-normalized diagram (Fig. 4a) is similar for all samples being moderately fractionated (Ce_N/Yb_N = 5.7–7.5). The REE patterns follow the pattern for the ACC, but with overall lower concentrations for the Lopaičiai-2 samples. All samples except for Lop2-46 and Lop2-45 show lowered concentrations of Eu. On the ACC-normalized diagram (Fig. 4b), the Lopaičiai samples display much more complicated trace-element patterns than the Dengtiltis samples. All Lopaičiai-2 samples are characterized by deep troughs at Ta–Nb, Ti and Co–Ni, and by slightly lowered Y concentrations. Both peat samples (Lop2-25 and Lop2-26) display very deep troughs at Zr–Hf and marked peaks at P. Sandy clay samples Lop2-45 and Lop2-46 display flat P distributions whereas the rest of the organic-poor samples show troughs at P. Samples Lop2-25 (peat), Lop2-35 (a transition between fine sand and dark-grey clay), Lop2-41, and Lop2-46 (both are sand) display very high concentrations of W (up to >10× ACC). Platinum group element signal intensities in the Lopaičiai sediments are variable with the lowermost intensities observed for peat samples (Fig. 8b).

3.3. Krokšlys

Nine samples from the depth interval of 75–195 cm were analyzed. Total amounts of trace elements in the studied samples

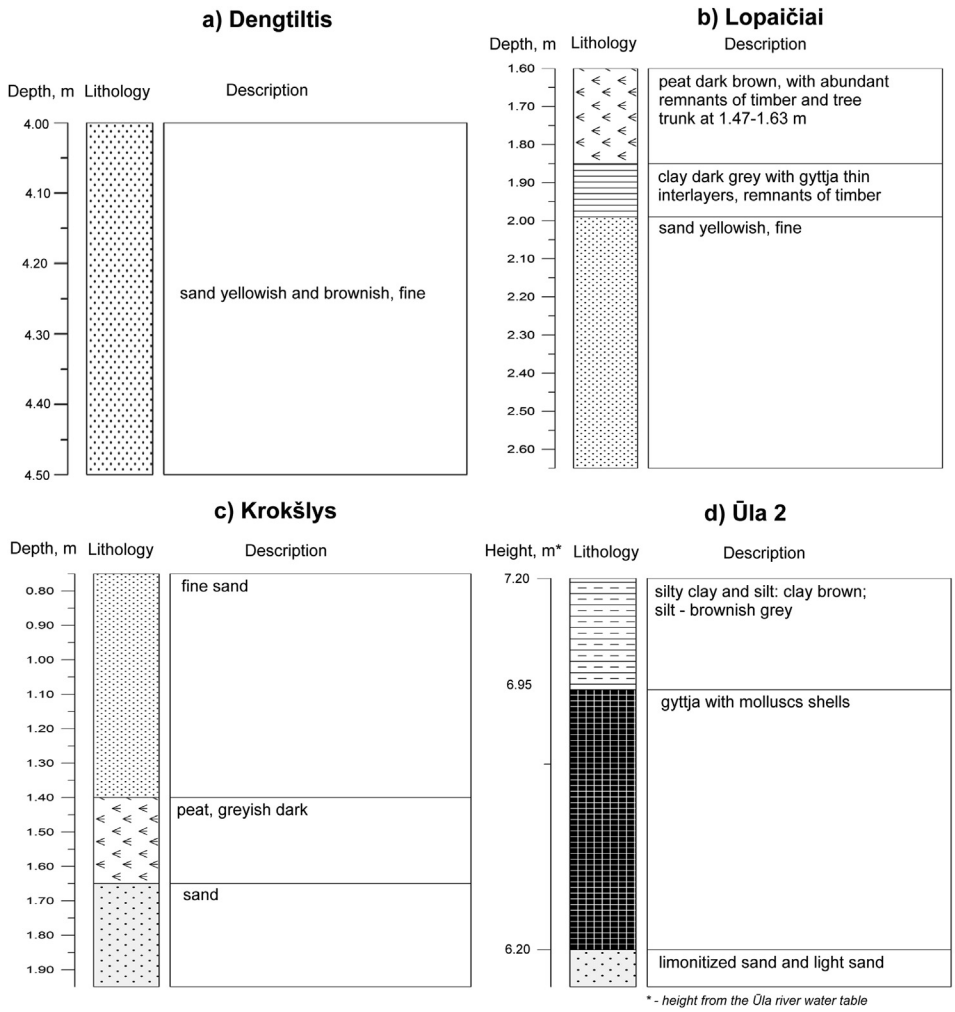

Fig. 2. Lithology of the studied sedimentary sequences: a, Dengtiltis; b, Lopaičiai-2; c, Krokšlys; d, Ūla-2.

are ~1000 ppm, i.e., up to four times lower than in the ACC. The REE patterns on a CI chondrite-normalized diagram (Fig. 5a) are similar for all samples in spite of the different lithologies, and are also very similar to those from the Dengtiltis outcrop (Fig. 3a). The patterns are moderately fractionated (Ce_N/Yb_N = 5.5–12.6) and generally follow the pattern style for the ACC, but with overall much lower REE concentrations for Krokšlys samples. On the ACC-normalized diagram (Fig. 5b), all Krokšlys samples display deep troughs at Ta–Nb, Ti, Y, and Co–Ni. Additionally, almost all samples (except for Kr-133, and Kr-135, both aeolian sand) are characterized by the elevated concentrations of Zr and Hf. All samples except for Kr-132 (peat) display peaks at Eu. Signal intensities of the PGE are very similar for almost all samples except for a sample Kr-131 (peat), which displays much stronger PGE signal intensities than other samples (Fig. 9b).

3.4. Ūla-2

Ten samples from the interval of 610–700 cm above the level of the Ūla River were analyzed. Total amounts of trace-elements vary from <700 ppm (for the middle part of the sequence) to up to ~2000 ppm (for the lowermost and uppermost parts of the sequence). The highest trace-element concentrations are displayed by samples Ula2-49 and Ula2-50 (yellowish sand) from the lowermost levels (610 and 620 cm, respectively), and by samples Ula2-64 and Ula2-66 (both gyttja) from the uppermost levels (690 and 700 cm, respectively). Overall, the REE distribution pattern styles for all Ūla-2 samples are similar to that of the ACC, displaying however lower concentrations and higher degrees of fractionation (Ce_N/Yb_N = 4.1–8.3; Fig. 6a) and troughs at Eu for samples Ula2-49 and Ula2-50. Samples from the middle and the uppermost parts of the sequence display peaks at Eu. Distributions of the trace-elements on the ACC-normalized diagram (Fig. 6b) are characterized by marked troughs at Ta–Nb and Ti, and slightly lowered concentrations of Y. Samples from a lower part of the sequence, and a sample Ula2-66 from the uppermost part of the sequence, display troughs at Co–Ni. All samples except for Ula2-49 and Ula2-50 (the lowermost part of the sequence) display elevated concentrations of W. All Ūla-2 samples except for samples Ula2-49, Ula2-50 and Ula2-66 are characterized by very low concentrations of U (U_N/Th_N = 1.5–1.8) as compared to the rest of the samples (U_N/Th_N = 4.0–32.9). Platinum group element signal intensities are low for most samples, but are elevated in samples Ula2-50 and Ula2-64 (Fig. 10b).

4. Discussion

4.1. Geochronological modeling

Our geochronological modeling is based on the combination of the age determinations (Table 2) and geochemical features of the

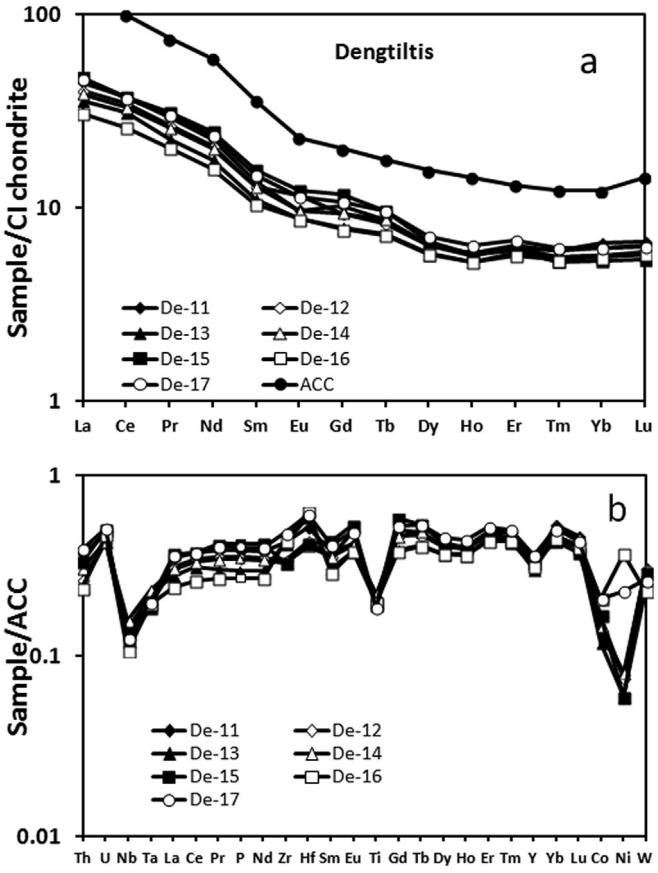

Fig. 3. Diagrams showing distribution of various trace elements in samples from the Dengtiltis outcrop: a, CI chondrite-normalized REE diagram (normalizing values are after Anders and Grevesse, 1989). A pattern for the ACC is given for a comparison; b, ACC-normalized trace element diagram (ACC values are after Wedepohl, 1995).

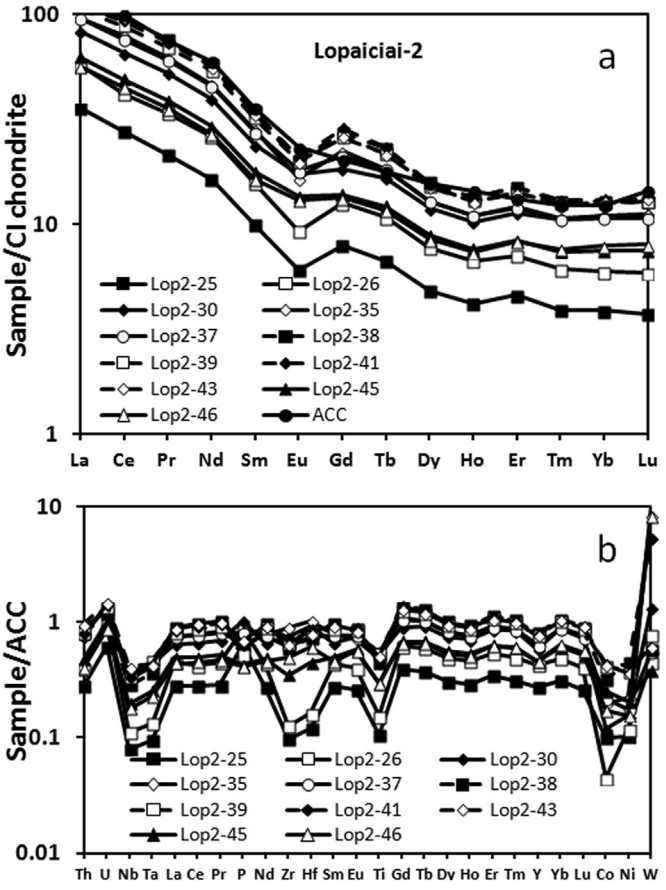

Fig. 4. Diagrams showing distribution of various trace elements in samples from the Lopaičiai-2 drilling site: a, CI chondrite-normalized REE diagram (normalizing values are after Anders and Grevesse, 1989). A pattern for the ACC is given for a comparison; b, ACC-normalized trace element diagram (ACC values are after Wedepohl, 1995).

sediments (Table 1). In addition to the available in literature age determinations, two samples from the outcrop Ūla-2 were dated by ^{14}C in the Poznań Radiocarbon Laboratory, Poland (No. 1 and 2 in Table 2). All radiocarbon ages were calibrated to calendar years BP using IntCal2013 calibration curve (Reimer et al., 2013) within the calibration software OxCal 4.2 (Bronk Ramsey, 2009) and are given as calibrated years before 1950 AD (cal BP).

Dengtiltis (Fig. 2a) sample from the level of 400 cm displays a thermo-luminescent (TL) age of 11,200 ± 1300 a BP, and a sample from the level of 450 cm an age of 14,100 ± 1500 a BP (Rudnickaitė et al., 2012). The following radiocarbon ages were obtained for samples from the Lopaičiai-2 drilling site (Fig. 2b): Lop2-25 (175 cm), 9495 ± 65 cal BP; Lop2-38 (220 cm), 12,487 ± 340 cal BP; Lop2-45 (260 cm), 12,900 ± 162 cal BP

Table 2
Absolute age determinations for Lithuanian samples.

A. Results of radiocarbon dating

No.	Height/Depth (cm)	Dated material	Laboratory code	^{14}C a BP	Calibrated age, cal BP (1σ interval)	After
Ūla-2						
1	695	Gyttja	Poz-44800	11,600 ± 60	13,417 ± 66 (68.2%)	This work
2	630	Gyttja	Poz-44802	12,660 ± 60	15,075 ± 121 (68.2%)	This work
Lopaičiai-2						
3	175	Peat	Vs-2111	8520 ± 90	9495 ± 65 (67.5%)	Kabailienė et al. (2014)
4	220	Clay	Vs-2115	10,680 ± 270	12,487 ± 340 (68.2%)	Kabailienė et al. (2014)
5	260	Clay	Vs-2116	11,030 ± 200	12,900 ± 162 (68.2%)	Kabailienė et al. (2014)

B. Results of thermo-luminescence (TL) dating

No.	Depth (cm)	Dated material	Laboratory code	TL age, a BP	After
Krokšlys					
6	75	Sand	UG-6515	9600 ± 2000	Dated by Fedorowicz in 2011
7	125	Sand	UG-6514	11,100 ± 2000	Dated by Fedorowicz in 2011
Dengtiltis					
8	400	Sand	UG-6124	11,200 ± 1300	Rudnickaitė et al. (2012)
9	450	Sand	UG-6125	14,100 ± 1500	Rudnickaitė et al. (2012)

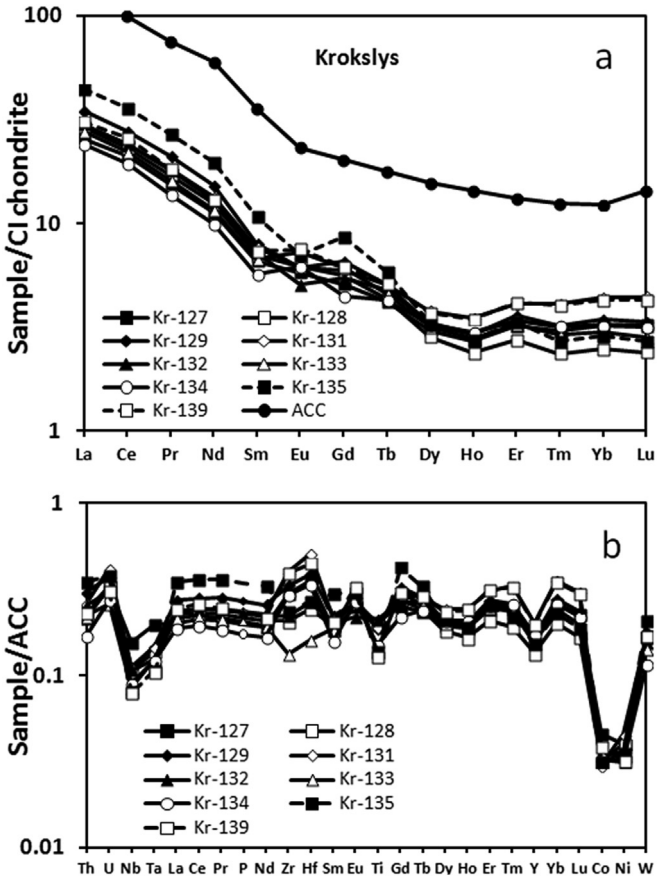

Fig. 5. Diagrams showing distribution of various trace elements in samples from the Krokšlys outcrop: a, CI chondrite-normalized REE diagram (normalizing values are after Anders and Grevesse, 1989). A pattern for the ACC is given for a comparison; b, ACC-normalized trace element diagram (ACC values are after Wedepohl, 1995).

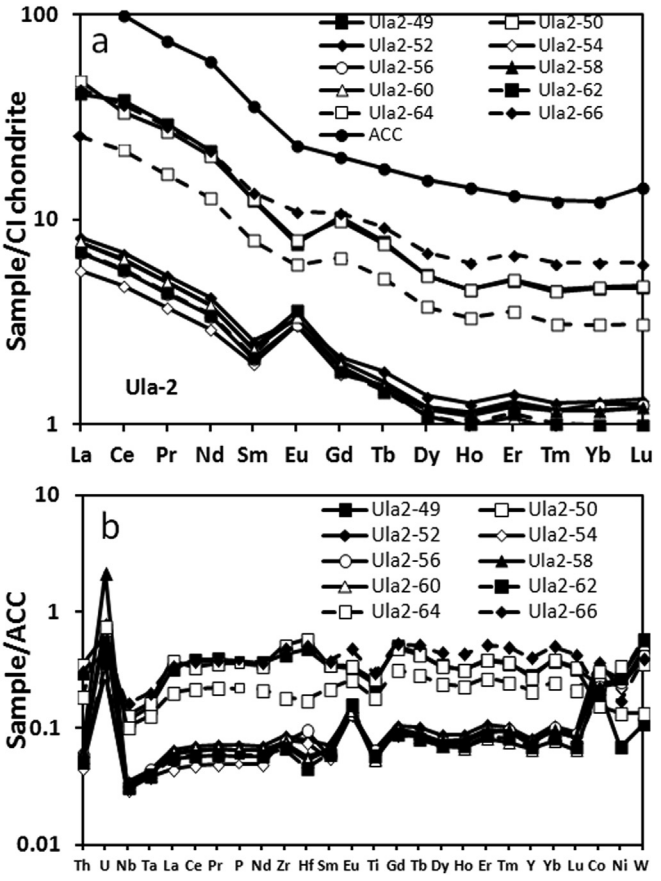

Fig. 6. Diagrams showing distribution of various trace elements in samples from the Ūla-2 outcrop: a, CI chondrite-normalized REE diagram (normalizing values are after Anders and Grevesse, 1989). A pattern for the ACC is given for a comparison; b, ACC-normalized trace element diagram (ACC values are after Wedepohl, 1995).

(Kabailienė et al., 2014). Krokšlys (Fig. 2c) sample from the level of 75 cm displays a TL age of 9600 ± 2000 a BP, and a sample from the level of 125 cm an age of 11,100 ± 2000 a BP (Analyzed by S. Fedorowicz, in 2011). There are two radiocarbon age determinations for the outcrop Ūla-2 (Fig. 2d): a sample from the level of 695 cm is dated as 13,417 ± 66 cal BP (Poz-44800), and a sample from the level of 630 cm (corresponds to sample Ula2-54) is dated as 15,075 ± 121 cal BP (Poz-44802).

Based on the geochemical features of the studied sediments, we detected a few geochemical markers. The first (the youngest) marker is detected for the Lopaičiai-2 sequence and is represented by Cu–Zn enrichment at the level of 180 cm (Fig. 8). As there is an age determination of 9495 ± 65 cal BP for sediments from the level of 175 cm (Table 2), we suggest that sediments enriched in Cu and Zn (located 5 cm below the level of 175 cm) roughly correspond to the age of 10.0 ka BP.

The second geochemical marker is identified for the Dengtiltis (410 cm), Krokšlys (155 cm), and Lopaičiai-2 (200 cm) sites (Fig. 7–9). The marker is pronounced in elevated concentrations of Ni for sediments from all three sites, Cr (Krokšlys), and Zr (Krokšlys and Lopaičiai-2 sites), and in elevated signal intensities for Ru, Ir and Pt for all three sites. Such similarities in the type of enrichment point, most likely, to the same event responsible for the addition of the named elements to the sediments. A time of enrichment can be deduced from the available age determinations (Table 2). The enriched deposits are located 10 cm below the level corresponding to the age of 11.2 ± 1.2 ka BP for Dengtiltis outcrop that, according to the average rate of sedimentation in the region, corresponds to the time difference of ~600 years. For Lopaičiai-2 drilling site, the enriched horizon is located 25 cm below the level corresponding to the age of 9495 ± 65 cal BP, and 25 cm above the level dated as 12,487 ± 340 cal BP. Therefore, the age of the enriched horizon should correspond to ca. 11.0 ka BP. Additionally, for Krokšlys outcrop, an enriched level is located below the level, which is dated by the TL method as 11,100 ± 2000 a BP. Therefore, we suggest that the enrichment took place approximately between 11.0 and 11.5 ka BP.

There are also two recognizable geochemical markers for sediments of the Ūla-2 sequence, which are older than sediments from the other three sequences (Table 2). The first (older) marker, pronounced in peaks at Cr, Zr, Hf and some REE, is observed in the lowermost part of the sequence (Fig. 10). Sediments from the lowermost part of the Ūla-2 sequence (below the 630 cm level) were deposited before 15,075 ± 121 cal BP (Poz-44802; Table 2). As the enrichment in the described elements is recognized at the level of 620 cm, i.e., 10 cm below the level dated as 15,075 ± 121 cal BP, we suggest an age of ca. 15.3 ka BP for the lower enriched horizon. The second marker is located at the level of 690 cm above the water level, and is pronounced in enrichment in Ni, Cu, Cr, and in the increased PGE intensity signals (Fig. 10). A similar type of the enrichment was also observed for the other three sites, but the ages are much younger there and are estimated as ca. 11.0–11.5 ka BP. On the other hand, for the studied part of the Ūla-2 sequence, the

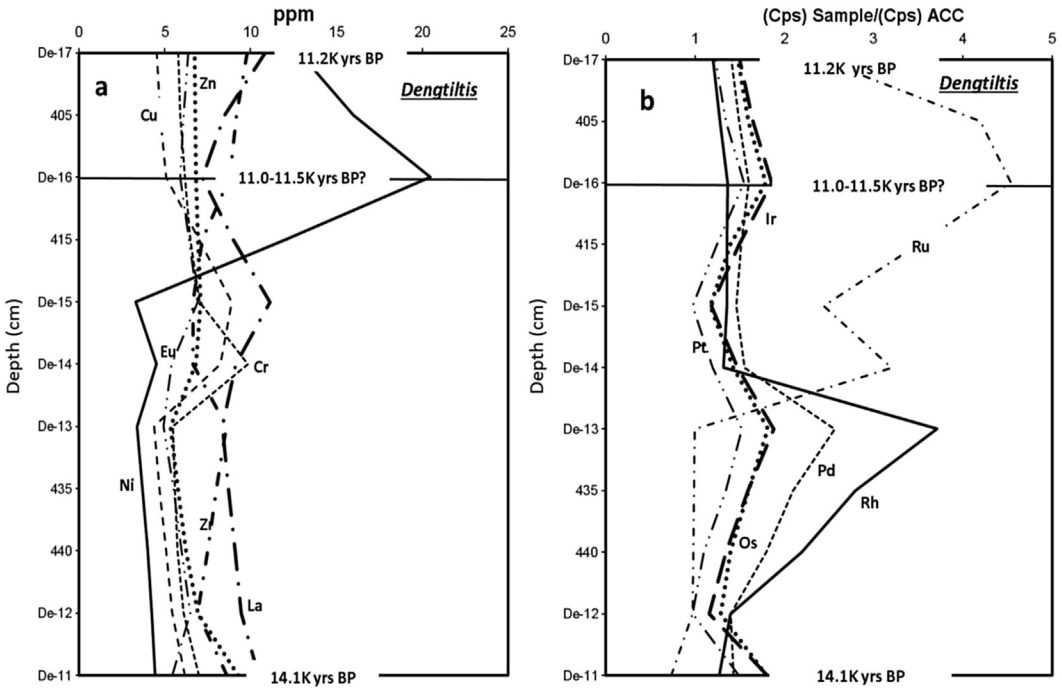

Fig. 7. Distribution of the selected trace elements (a) and PGE (b) across the studied part of the sedimentary sequence of the Dengtiltis outcrop. Trace element concentrations in (a) are given in ppm as: Cr/1; Ni/1; Cu/1; Zr/10; La/1; Eu*10; Zn/2. The PGE are given in signal intensities (Cps) normalized to such intensities for samples of the ACC (see text for details). The ages of 11.2 ka and 14.1 ka BP are after Rudnickaitė et al. (2012). A solid black line marks stratigraphic levels corresponding to the time of a suggested local ET event, which might have occurred ca. 11.0–11.5 ka BP; see text for more details.

enrichment of this type is older with the radiocarbon age determination of 13,417 ± 66 cal BP (Poz-44802; Table 2) for sediments from the level of 695 cm. Therefore, the age of the enriched sediments, which are located 5 cm below, can be estimated as ca. >13.5 ka BP.

4.2. Interpretations of geochemical features

A close similarity of the REE patterns is evident for samples from Dengtiltis and Krokšlys sites (Figs. 3a and 5a). Rare earth elements patterns for sediments from both sites are characterized by lower

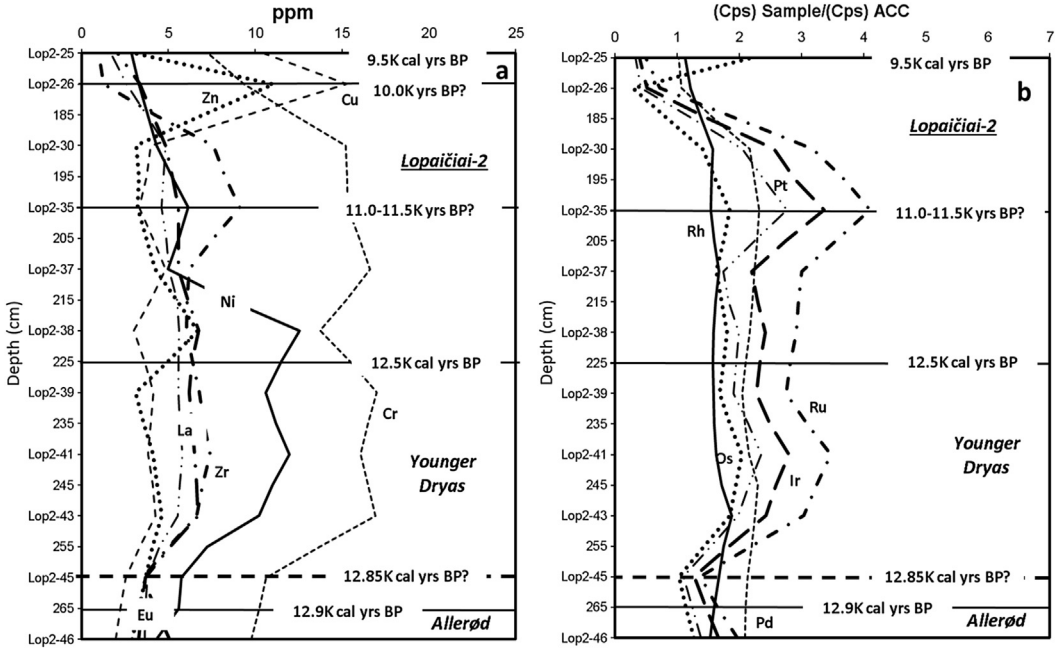

Fig. 8. Distribution of the selected trace elements (a) and PGE (b) across the studied part of the sedimentary sequence of the Lopaičiai-2 drilling site. Trace element concentrations in (a) are given in ppm as: Cr/2; Ni/2; Cu/4; Zr/20; La/42; Eu*5; Zn/20. The PGE are given in signal intensities (Cps) normalized to such intensities for samples of the ACC (see text for details). The age of 9.5 ka cal BP, 12.5 ka cal BP, and 12.9 ka cal BP after Kabailienė et al. (2014). The dashed black line (age of 12.85 ka cal BP; Kabailienė et al., 2011) marks a suggested location of the lower YD boundary. The level with the suggested age of 11.0–11.5 ka BP corresponds to the time of a suggested local ET event; see text for details.

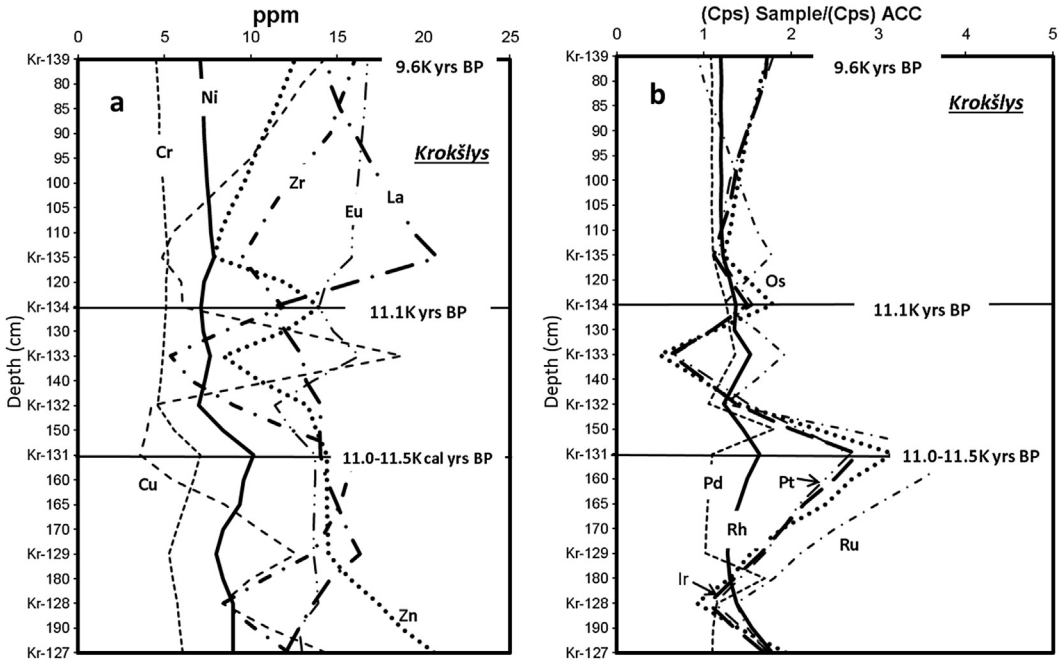

Fig. 9. Distribution of the selected trace elements (a) and PGE (b) across the studied part of the sedimentary sequence of the Krokšlys outcrop. Trace element concentrations in (a) are given in ppm as: Cr/1; Ni*5; Cu*5; Zr/5; La*2; Eu*40; Zn*1.5. The PGE are given in signal intensities (Cps) normalized to such intensities for samples of the ACC (see text for details). The ages of 9.6 ka BP and 11.1 ka BP are TL dates obtained by S. Fedorowicz in 2011. A solid black line marks stratigraphic levels corresponding to the time of a suggested local ET event, which might have occurred ca. 11.0–11.5 ka BP; see text for more details.

than the ACC concentrations and moderate degrees of fractionation. Moreover, normalized to the ACC trace-element diagrams for both sites are also very similar and display such common for most samples features as troughs at Nb–Ta and Co–Ni, and enrichment in Zr–Hf. All these features combined together suggest a similar source of material for sediments for these two sites.

One of the geochemical markers detected for the Lopaičiai-2 sediments is characterized by high concentrations of Cu and Zn that suggests the presence of abundant Cu–Zn sulfides? in sediments corresponding to the age of ca. 10.0 ka BP. This marker was observed for only one of the studied sequences, and can be considered as a restricted local feature, whose nature is unclear. Some geochemical

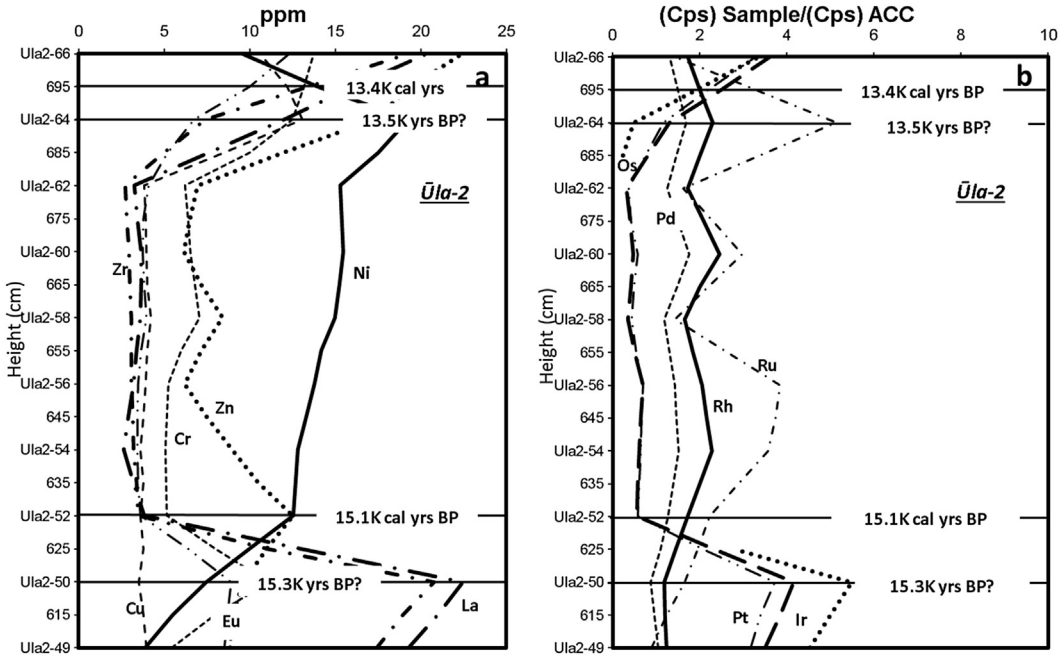

Fig. 10. Distribution of the selected trace elements (a) and PGE (b) across the studied part of the sedimentary sequence of the Ūla-2 outcrop. Trace element concentrations in (a) are given in ppm as: Cr/1; Ni/1; Cu/1; Zr/5; La*2; Eu*20; Zn/1. The PGE are given in signal intensities (Cps) normalized to such intensities for samples of the ACC (see text for details). The age of 13.4 ka cal BP is a sample Poz-44800 (this work), 15.1 ka cal BP is a sample Poz-44802 (this work). The level of 620 cm corresponds to the time of 15.3 ka BP and contains volcanic material, which might have originated from the eruption of one of the volcanoes of Chaîne des Puys volcanoes, French Massif Central (Juvigné et al., 1994; Vernet et al., 1998); see text for details. The level with the suggested age of 13.5 ka BP corresponds to the time of the second suggested local ET event; see text for details.

features of the studied sediments allow us to suggest that small amounts of volcanic and meteoritic components are present in the sediments from selected stratigraphic levels.

4.2.1. Volcanic component

It is known that Pleistocene was a time of high volcanic activity in Europe. Overall, presence of volcanic material in sediments can be identified on the basis of the presence of microscopic shards of volcanic glass and/or minerals, and also on the basis of geochemical features of sediments (cf. Subetto et al., 2002; Subetto, 2009; Andronikov et al., 2014). Products of volcanic eruptions are commonly enriched in such "volcanic" elements as REE, Zr and Hf, and their elevated concentrations in sediments suggest a presence of the volcanic material. Elevated concentrations of such "volcanic" elements as Zr, Hf and REE for the lowermost part of the Ūla-2 sequence (sample Ula2-50; 620 cm above the water level; Fig. 10) allows us to suggest here the presence of the volcanic component. A part of the section where the enriched horizon is located, deposited according to our geochronological model ca. 15.3 ka cal BP. This age coincides with the time of the earliest eruptions of Chaîne des Puys volcanoes, French Massif Central (Juvigné et al., 1994; Vernet et al., 1998). Although Lithuania is located a distance away from the Massif Central, the volcanic material can, under favorable atmospheric conditions, travel for long distances. For example, the presence of Vedde Ash (12.1 ka cal BP; Lane et al., 2012) from the eruption of the Icelandic volcano Katla is known in sediments of Lake Medvedevskoye from NW Russia (Subetto et al., 2002; Subetto, 2009). Therefore, the presence of volcanic material from the French Massif Central in Lithuanian sediments is not something extraordinary and completely unexpected.

4.2.2. Meteoritic component

Some elements, whose concentrations are much higher in meteorites than in terrestrial materials ("meteoritic" elements) could be considered as indicators of the presence of ET material (Anders and Grevesse, 1989; Wedepohl, 1995; Lorand et al., 2008). Overall, in studies related to meteorite impacts, an increase of the PGE concentrations suggests to be a clear indicator of a contribution of meteoritic component to the terrestrial environment (e.g., Alvarez et al., 1980; Sawlowicz, 1993; Palme, 2008). This is because concentrations of the PGE in meteoritic material are about four orders of magnitude higher than in the ACC (450 ppb and <0.1 ppb, respectively; Anders and Grevesse, 1989; Wedepohl, 1995). However, enrichment in any "meteoritic" element alone could be explained by terrestrial processes (changes in a source of sedimentary material or influence of biotic activity), and only simultaneous enrichment in a few "meteoritic" elements should raise suspicion about the presence of the ET-related material.

The sediments enriched in such "meteoritic" elements as Ni, Cr, and some PGE were observed in all studied sequences. According to our geochronological model, the youngest horizon enriched in "meteoritic" elements is observed in three out of four studied sequences and corresponds to the age of ca. 11.0–11.5 ka BP. We suggest that this geochemical marker is resulted from a meteoritic impact. We tentatively connect this feature with a Velnio Duobės (Devil's Hole; N 54°35′; E 24°31′) meteorite structure in South Lithuania (Fig. 1), which formed before 10 ka BP (Gailius and Karmaza, 2013). There is also information on a meteorite impact crater(s) of similar age in Estonia (Tsöörikmäe structure; N 58°06′; E 27°30′) (Pirrus and Tiirmaa, 1985).

The Ūla-2 sequence displays enrichment in "meteoritic" elements at the level which corresponds to ca. >13.5 ka BP according to our geochronological model (Fig. 10). This type of enrichment is very similar to that of the other three localities in spite of almost two thousand years time difference between Ūla-2 and the rest of the sediments. Therefore, enrichment of sediments of ca. 13.5 ka BP and ca. 11.0–11.5 ka BP was due to similar events, i.e., meteorite impact. As there is no information on meteorite craters of the age of ca. 13.5 ka cal BP in the region, it is possible that we deal here with the fingerprints of a bolide airburst or alternatively the impact could occur on the Ice Sheet, therefore, not making a visible crater.

Only one of the studied sites (Lopaičiai-2 drilling site) covers a time interval transitional between Allerød and Younger Dryas, i.e., the time suggested by Firestone et al. (2007) for a catastrophic pre-YD ET event. The geochemical characteristics of the Lopaičiai-2 sediments changed shortly after ca. 12.9 ka cal BP, which is reflected in an increase in concentrations of both "volcanic" and "meteoritic" elements (Fig. 8). However, this increase is not pronounced in a clear peak at element concentrations, but rather is steady, with elevated concentrations of some elements for an extended period of time (for almost a thousand years, according to our geochronological model). We suggest that both volcanic and meteoritic components were added to the Lopaičiai-2 sediments almost simultaneously just before the onset of the Younger Dryas climate oscillation. It is known that shortly before the beginning of the YD cooling, the Laacher See volcano (Eifel, Germany) erupted (e.g., Ammann and Lotter, 1989; van den Bogaard, 1995; Brauer et al., 1999; Pissart, 2003; Riede, 2007). This eruption was one of the most significant volcanic events of the Late Pleistocene in Northern Europe with >6 km^3 of magmatic material explosively erupted, covering an area of ~1300 km^2 in lava and ash deposits (Wörner and Schmincke, 1984; van den Bogaard and Scmincke, 1985; van den Bogaard, 1995; Riede, 2007). The timing of this eruption is 12,880 a BP (Brauer et al., 1999; Litt et al., 2001; Lane et al., 2011), virtually indistinguishable from the age estimated for enriched in "volcanic" elements of Lopaičiai-2 sediments. Therefore, this suggests the presence of the Laacher See volcanic material in the Lithuanian sediments. A presence of the meteoritic component in the Lopaičiai-2 sediments can be provisionally connected with the pre-YD (12.9–12.8 ka BP) ET event suggested by Firestone et al. (2007). However, as the presence of the meteorite component is very subtle, we cannot conclude unequivocally on the basis of the available geochemical features whether a catastrophic pre-YD ET event really took place, rather than another local ET event.

The long-term existence of elevated concentrations of the elements-markers in the sediments requires a presence of a long-existing source for such elements. During the Late Pleistocene, the studied region was located in the vicinity of the continental glacier (e.g., Thomson, 1995; Svendsen et al., 2004; Kalm, 2012), which served as the main source for streams feeding the lakes of the region. It is known that ice sheets are good collectors of various airborne microparticles. If such microparticles resulted either from the ET impact/explosion, volcanic eruption, or both deposited on the glacier (a prominent elevated feature of the relief in the Late Pleistocene), because of the dark color, they would be easily heated by solar radiation and incorporated into the ice down to some different (depending on the particle's size and physical properties) depths enriching. Continuing seasonal melting of the ice containing incorporated ET/volcanic particles might have provided the enriching component(s) for the region of sedimentation (Late Pleistocene lakes of Lithuania) for an extended period of time.

5. Conclusions

Most studied sedimentary sequences in Lithuania are lithologically inhomogeneous and are characterized by uneven distribution of trace-elements across the sequences. Conducted geochronological modeling suggests that the studied parts of sedimentary sequences were deposited during a time period from Bølling to Younger Dryas. Changes in geochemical characteristics are mostly

due to the changes in lithology and conditions of sediment deposition. It follows from the geochemical features that the material for sediments from the Dengtiltis and Krokšlys sequences was delivered from the same or a very similar source. Although most geochemical features are due to different lithologies of the studied sediments, some features are inconsistent with a change of lithology, and require other explanations. We were able to reveal geochemical fingerprints of a meteoritic component that could be due to the ET event of ca. 11.0–11.5 ka BP for three out of the four studied sedimentary sequences, and of ca. 13.5 ka BP for the Ūla-2 sequence. The younger event was likely a local meteorite impact which might have resulted in Velnio Duobės meteorite crater (South Lithuania). The event of ca. 13.5 ka BP was, likely, pronounced as the airburst, as judged from the absence of a meteorite crater of this or similar age in the region. The presence of volcanic material was detected for the Ūla-2 sequence at the stratigraphic levels corresponding to the age of ca. 15.3 ka cal BP. We relate these materials to the beginning of the eruption of the Chaîne des Puys volcanoes, French Massif Central.

We also suggest, that sediments from the Lopaičiai-2 drilling site contain minute amounts of volcanic and meteoritic materials at the levels just above that corresponding to the age of 12,900 ± 162 cal BP. The volcanic material from this site can be related to the eruption of the Laacher See volcano (12.88 ka BP). On the other hand, so far we cannot unequivocally confirm or disconfirm whether meteoritic material in the Lopaičiai-2 sediments existing at the same stratigraphic level as the Laacher See volcanic material is related to the pre-YD ET event suggested by Firestone et al. (2007). The applied geochemical methodology, if confirmed by further research on additional sequences, could potentially be used as an additional tool for correlation between different Late Pleistocene records for a period during which radiocarbon dating still contains uncertainties.

Acknowledgments

We thank C. V. Haynes, J. Ballenger, A. van Hoesel, W. Hoek, M. Drury, D.A. Subetto, C. Verbruggen and N. van den Putten for very fruitful discussions on the considered issues, and S. Fedorowicz for TL dating of two Krokšlys samples. We also would like to thank reviewers for their valuable comments, which helped to improve this paper. This study was supported in part by the NAI International Collaboration Fund for AVA. Field work and radiocarbon dating was financed by the Research Council of Lithuania, project LEK-03/2010.

References

Alley, R.B., 2000. The Younger Dryas cold interval as viewed from central Greenland. Quaternary Science Reviews 19, 213–226.
Alvarez, L.W., Alvarez, W., Asaro, F., Michel, H.V., 1980. Extraterrestrial cause for the Cretaceous-Tertiary extinction. Science 208, 1095–1108.
Ammann, B., Lotter, A.F., 1989. Late-Glacial radiocarbon- and palynostratigraphy on the Swiss Plateau. Boreas 18, 109–126.
Anders, E., Grevesse, N., 1989. Abundances of the elements: meteoritic and solar. Geochimica et Cosmochimica Acta 53, 197–214.
Andronikov, A.V., Lauretta, D.S., Subetto, D.A., Andronikova, I.E., Drosenko, D.A., Kuznetsov, D.D., Sapelko, T.V., Syrykh, L.A., 2014. In search for fingerprints of an extraterrestrial event: trace element characteristics of sediments from the Lake Medvedevskoye (Karelian Isthmus, Russia). Doklady Earth Sciences 457, 819–823.
Artemieva, N., Morgan, J., 2009. Modeling the formation of the K–Pg boundary layer. Icarus 201, 768–780.
Beets, C., Sharma, M., Kasse, K., Bohncke, S., 2008. Search for Extraterrestrial Osmium at the Allerod – Younger Dryas Boundary. American Geophysical Union. Fall Meeting 2008, Abstract V53A-2150.
Berger, W.H., 1990. The Younger Dryas cold spell – a quest for causes. Global Planet Change 3, 219–237.
Björck, S., 2007. Younger Dryas Oscillation, Global Evidence. In: Scott, A.E. (Ed.), Encyclopedia of Quaternary Science. Elsevier, Oxford, pp. 1983–1995.
van den Bogaard, P., 1995. $^{40}Ar/^{39}Ar$ ages of sanidine phenocrysts from Laacher See Tephra (12,900 yr BP): chronostratigraphic and petrological significance. Earth and Planetary Science Letters 133, 163–174.
van den Bogaard, P., Schmincke, H.-U., 1985. Laacher See Tephra: a widespread isochronous late Quaternary tephra layer in central and northern Europe. Geological Society of America Bulletin 96, 1554–1571.
Brauer, A., Enders, C., Negendank, J.F.W., 1999. Lateglacial calendar year chronology based on annually laminated sediments from Lake Meerfelder Maar, Germany. Quaternary International 61, 17–25.
Brauer, A., Haug, G.H., Dulski, P., Sigman, D.M., Negendank, J.F.W., 2008. An abrupt wind shift in Western Europe at the onset of the Younger Dryas cold period. Nature Geoscience 1, 520–523.
Bronk Ramsey, C., 2009. Bayesian analysis of radiocarbon dates. Radiocarbon 51, 337–360.
Bunch, T.E., Wittke, J.H., West, A., Kennett, J., Kennett, D.J., Que Hee, S.S., Wolbach, W.S., Stich, A., Mercer, C., Weaver, J.C., 2008. Hexagonal diamonds (lonsdaleite) discovered in the K/T impact layer in Spain and New Zealand. In: AGU Fall Meeting, Abstract PP13C-1476, Eos Transactions 89.
Bunch, T.E., Hermes, R.E., Moore, A.M.T., Kennett, D.J., Weaver, J.C., Wittke, J.H., DeCarli, P.S., Bischoff, J.L., Hillman, G.C., Howard, G.A., Kimbel, D.R., Kletetschka, G., Lipo, C.P., Sakai, S., Revay, Z., West, A., Firestone, R.B., Kennett, J.P., 2012. Proceedings of the National Academy of Science 109, 1903–1912.
Firestone, R.B., West, A., Kennett, J.P., Bunch, T.E., Revay, Z.S., Schultz, P.H., Belgya, T., Kennett, D.J., Erlandson, J.M., Dickenson, O.J., Goodyear, A.C., Harris, R.S., Howard, G.A., Kloosterman, J.B., Lechler, P., Mayewski, P.A., Montgomery, J., Poreda, R., Darrah, T., Que Hee, S.S., Smith, A.R., Stich, A., Topping, W., Wittke, J.H., Wolbach, W.S., 2007. Evidence for an extraterrestrial impact 12,900 years ago that contributed to the megafaunal extinctions at the Younger Dryas cooling. Proceedings of the National Academy of Science 104, 16016–16021.
Gailius, R., Karmaza, B., 2013. Devil's Hole – other approach and facts. Geologijos akiračiai 4, 27–36 (in Lithuanian with English summary).
van Hoesel, A., Hoek, W., Braatbaard, F., van der Plicht, H., Pennock, J.M., Drury, M.R., 2012. Nanodiamonds and wildfire evidence in the Usselo horizon postdate the Allerød-Younger Dryas boundary. Proceedings of the National Academy of Science 109, 7648–7653.
van Hoesel, A., Hoek, W.Z., Pennock, G.M., Drury, M.R., 2014. The Younger Dryas impact hypothesis: a critical review. Quaternary Science Reviews 83, 95–114.
Isarin, R.F.B., Renssen, H., 1999. Reconstructing and modeling Late Weichselian climates: the Younger Dryas in Europe as a case study. Earth Science Reviews 48, 1–38.
Israde-Alcántara, I., Bischoff, J.L., Domíniguez-Vásquez, G., Li, H.-C., DeCarli, P.S., Bunch, T.E., Wittke, J.H., Weaver, J.C., Firestone, R.B., West, A., Kennett, J.P., Mercer, C., Xie, S., Richman, E.K., Kinzie, C.R., Wolbach, W.S., 2012. Evidence from Central Mexico supporting the Younger Dryas extraterrestrial impact hypothesis. Proceedings of the National Academy of Science 109, E738–E747.
Juvigné, E., Bastin, B., de Goer, B., de Herve, A., 1994. Nouvelles donnees sur les tephras et l'environnment tardiglaciaires du cezalier et de L'Artense (Massif Central, France). Annales de la Société géologique de Belgique 117, 321–332.
Kabailienė, M., Rudnickaitė, E., Macijauskaitė, L., Balakauskas, L., 2011. Vegetation dynamics during Younger Dryas climatic episode (12600–11500 yr. cal. B.P.). In: Northwest Lithuania. XXVIII INQUA Congress: Quaternary Sciences – the View from the Mountains, 21–27 July 2011, Bern, Switzerland. ID 997.
Kabailienė, M., Vaikutienė, G., Macijauskaitė, L., Šinkūnas, P., Rudnickaitė, E., Kisielienė, D., Gruguc, G., 2014. Late Glacial and Holocene vegetation and environmental changes at Lopaiciai and Pakastuva, NW Lithuania. Quaternary International (in this volume).
Kalm, V., 2012. Ice-flow pattern and extent of the last Scandinavian Ice Sheet southeast of the Baltic Sea. Quaternary Science Review 44, 51–59.
Lane, C.S., Blockley, S.P.E., Lotter, A.F., 2011. Tephrochronology and absolute centennial scale synchronisation of European and Greenland records for the last glacial to interglacial transition: a case study of Soppensee and NGRIP. Quaternary International 246, 145–156.
Lane, C.S., Blockley, S.P.E., Mangerud, J., Smith, V.C., Lohne, Ø.S., Tomlinson, E.L., Matthews, I.P., Lotter, A.F., 2012. Was the 12.1 ka Icelandic Vedde Ash one of a kind? Quaternary Science Review 33, 87–99.
LeCompte, M.A., Goodyear, A.C., Demitroff, M.N., Batchelor, D., Vogel, E.K., Mooney, C., Rock, B.N., Seidel, A.W., 2012. Independent evaluation of conflicting microspherule results from different investigations of the Younger Dryas impact hypothesis. Proceedings of the National Academy of Science 109, E2960–E2969.
Litt, T., Brauer, A., Goslar, T., Merkt, J., Balaga, K., Müller, H., Ralska-Jasiewiczowa, M., Stebich, M., Negendank, J.F.W., 2001. Correlation and synchronisation of Late-glacial continental sequences in northern central Europe based on annually laminated lacuistrine sediments. Quaternary Science Reviews 20, 1233–1249.
Lorand, J.-P., Lufuet, A., Alard, O., 2008. Platinum-group elements: a new set of key tracers for the Earth's interior. Elements 4, 247–252.
Lowe, J.J., Rasmussen, S.O., Björck, S., Hoek, W.Z., Steffensen, J.P., Walker, M.J.C., Yu, Z.C., INTIMATE group, 2008. Synchronisation of palaeoenvironmental events in the North Atlantic region during the Last Termination: a revised protocol recommended by the INTIMATE group. Quaternary Science Reviews 27, 6–17.
McManus, J.F., Francois, R., Gherardi, J.-M., Keigwin, L.D., Brown-Legar, S., 2004. Collapse and rapid resumption of Atlantic meridianal circulation linked to deglacial climate changes. Nature 428, 834–837.

Marshall, W., Head, K., Clough, R., Fisher, A., 2011. Exceptional iridium concentrations found at the Allerød-Younger Dryas transition in sediments from Bodmin Moor in southwest England. In: Abst XVIII INQUA Congress 21–27 July 2011 Bern, Switzerland (ID 2641).

Murton, J.B., Bateman, M.D., Dallirmore, S.R., Teller, J.T., Yang, Z., 2010. Identification of Younger Dryas outburst flood path from Lake Agassiz to the Arctic Ocean. Nature 464, 740–743.

Palme, H., 2008. Platinum-group elements in Cosmochemistry. Elements 4, 233–238.

Peteet, D., 1995. Global Younger Dryas? Quaternary International 28, 93–104.

Pinter, N., Scott, A.C., Daulton, T.L., Podoll, A., Koeberl, C., Anderson, R.S., Ishman, S.E., 2011. The Younger Dryas impact hypothesis: a requiem. Earth Science Reviews 106, 247–264.

Pirrus, E.A., Tiirmaa, R.T., 1985. Tsöörikmägi – probably new meteorite crater in Estonia. Meteoritika 44, 141–149 (in Russian).

Pissart, A., 2003. The remnants of Younger Dryas lithalsas on the Hautes Fagnes Plateau in Belgium and elsewhere in the world. Geomorphology 52, 5–38.

Reimer, P.J., Bard, E., Bayliss, A., Beck, J.W., Blackwell, P.G., Bronk Ramsey, C., Buck, C.E., Cheng, H., Edwards, L., Friedrich, M., Grootes, P.M., Guilderson, T.P., Haflidason, H., Hajdas, I., Hatté, C., Heaton, T.J., Hoffmann, D.L., Hogg, A.G., Hughen, K.A., Kaiser, K.F., Kromer, B., Manning, S.W., Niu, M., Reimer, R.W., Richards, D.A., Scott, E.M., Southon, J.R., Staff, R.A., Turney, C.S.M., van der Plicht, J., 2013. IntCal13 and Marine13 radiocarbon age calibration curves 0–50,000 Years cal BP. Radiocarbon 55, 1869–1887.

Riede, F., 2007. Der Ausbruch des Laacher See-Vulkans vor 12.920 Jahren und urgeschichtlicher Kulturwande am Ende des Alleroed. Eine neue Hypothese zum Ursprung der Bromme-Kultur und des Purstunien. Mitteilungen der Gesellschaft fuer Urgeschichte 16, 25–54.

Rudnickaitė, E., Fedorowicz, S., Kaminskas, D., Melešytė, M., 2012. Geochronological sequence of paleogeographical variation in Northern Lithuania based on Dengtiltis outcrop (Dubysa river valley) studies. In: Abstracts of the International Conference "Geomorphology and Quaternary Paleogeography of Polar Regions. Herzen Pedagogical University Press, St. Petersburg, pp. 463–465.

Sawlowicz, Z., 1993. Iridium and other platinum-group elements as geochemical markers in sedimentary environments. Palaeogeography, Palaeoclimatology, Palaeoecology 104, 253–270.

Subetto, D.A., 2009. Lake sediments: Paleolimnological Reconstructions. A. Herzen Russian State Pedagogical University, Saint Petersburg, 333 p. (in Russian).

Subetto, D.A., Wohlfarth, B., Davydova, N.N., Sapelko, T.V., Björkman, L., Solovieva, N., Wastegård, S., Possnert, G., Khomutova, V.I., 2002. Climate and environment on the Karelian Isthmus, northwestern Russia, 13000–9000 cal. yrs BP. Boreas 31, 1–19.

Svendsen, J., Alexanderson, H., Astakhov, V.I., Demidov, I., Dowdeswell, J.A., 2004. Late Quaternary ice sheet history of Eurasia. Quaternary Science Reviews 23, 1229–1271.

Teller, J.T., Leverington, D.W., Mann, J.D., 2002. Freshwater outbursts to the ocean from glacial Lake Agassiz and their role in climate change during the last deglaciation. Quaternary Science Reviews 21, 879–887.

Thomson, J., 1995. Ice age terrestrial carbon change revisited. Global Biogeochemical Cycles 9, 377–389.

Tian, H., Schryvers, D., Clayes, Ph, 2010. Nanodiamonds do not provide unique evidence for a Younger Dryas impact. Proceedings of the National Academy of Science 108, 40–44.

Vernet, G., Raynal, J.P., Fain, J., Miallier, D., Montret, M., Pilleyre, T., Sanzelle, S., 1998. Tephrostratigraphy of the last 160 ka in Western Limagne (France). Quaternary International 47/48, 139–146.

Wedepohl, K.H., 1995. The composition of the continental crust. Geochimica et Cosmochimica Acta 59, 1217–1232.

Wittke, J.H., Weaver, J.C., Bunch, T.E., Kennett, J.P., Kennett, D.J., Moore, A.M.T., Hillman, G.C., Tankersley, K.B., Goodyear, A.C., Moore, C.R., Daniel Jr., R., Ray, J.H., Lopinot, N.H., Ferraro, D., Israde-Alcántara, I., Bischoff, J.L., DeCarli, P.S., Hermes, R.E., Kloosterman, J.B., Revay, Z., Howard, G.A., Kimbel, D.R., Kletetschka, G., Nabelek, L., Lipo, C.P., Sakai, S., West, A., Firestone, R.B., 2013. Evidence for deposition of 10 million tonnes of impact spherules across four continents 12,800 y ago. Proceedings of the National Academy of Science 110, E2088–E2097.

Wörner, G., Schmincke, H.-U., 1984. Mineralogical and chemical zonation of the Laacher See Tephra sequence (East Eifel, W. Germany). Journal of Petrology 25, 805–835.

Wu, Y., Sharma, M., LeCompte, M.M., Demitroff, M.N., Landis, J.D., 2013. Origin and provenance of spherules and magnetic grains at the Younger Dryas Boundary. Proceedings of the National Academy of Science 110, E3557–E3566.